Self Energy effect in frequency dependent Vertex flow equation

D. Vilardi,[1] C. Taranto,[1] and W. Metzner[1]

[1] *Max Planck Institute for Solid State Research, Stuttgart*
(Dated: June 19, 2017)

blablabl ...

PACS numbers:

I. INTRODUCTION

Introduction bla bla

II. FORMALISM

A. Model

The Hubbard model[1] describes spin-$\frac{1}{2}$ fermions with a density-density interaction:

$$\mathcal{H} = \sum_{i,j,\sigma} t_{ij} c_{i,\sigma}^{\dagger} c_{j,\sigma} + U \sum_i n_{i,\uparrow} n_{i,\downarrow} \qquad (1)$$

where $c_{i,\sigma}^{\dagger}$ and $c_{i,\sigma}$ are, respectively, creation and annihilation operators for fermions with spin $\sigma = \uparrow, \downarrow$. We consider the two-dimensional case with square lattice and repulsive interaction $U > 0$ at finite temperature T and in the SU(2) spin-symmetric phase. The hopping amplitude is restricted to $t_{ij} = t$ for nearest neighbors, $t_{ij} = t'$ for next-to-nearest neighbors.

B. Flow equations

In the following paragraph we will give some details about the functional renormalization group[2,3], and we will clarify some notation issue about the vertex.

Generally speaking, the fRG allows to use the renormalization group idea in the functional integral formalism. This is done by endowing the non-interacting propagator G_0, and hence the action, with an additional dependence on a scale parameter Λ, which generates an exact functional flow equation[4] with known initial conditions. The final result is recovered for some final Λ-value so that: $G_0^{\Lambda_f} = G_0$.

We will apply this approach to the effective action, whose expansions into the fields generates the one-particle irreducible (1PI) functions. By expanding the functional flow equation, one obtains a hierarchy of flow equations for the 1PI functions, involving vertexes of arbitrarily high orders. We will restrict ourselves to the two-particle level truncation by retaining only the two lowest nonvanishing orders in the expansion, i.e., we consider the flow of the self-energy Σ^Λ and of the two-particle
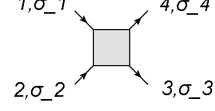

Figure 1: Notation of the two-particle vertex.

1PI vertex V^Λ, neglecting the effects of higher order vertexes. This truncation restricts the applicability of the approach to the weak-to-moderate coupling regime[5]. It can be furhter shown that, at the two-particle level trunctaion, the fRG sums up efficiently, although approximately, the so-called parquet-diagrams[6–8].

Due to translational invariance, we use the energy and momentum conservation to fix one of the arguments of the self energy and of the vertex. Due to SU(2) symmetry, for the self-energy we only need to consider one function depending on one frequency-momentum argument:

$$\Sigma_{\sigma\sigma'}^{\Lambda}(k) = \Sigma(k)\delta_{\sigma,\sigma'}, \qquad (2)$$

where $\sigma = \{\uparrow, \downarrow\}$, and $k = (\nu, \mathbf{k})$, ν being a fermionic Matsubara frequency and $\mathbf{k}$ a momentum in the first Brillouin zone.

For the notation of the two-particle vertex we refer to Fig. 1, where $k_i = (\nu_i, \mathbf{k_i})$, and $k_4 = k_1 + k_2 - k_3$. Furthermore SU(2)-symmetry guarantees that the vertex does not vanish only for six spin combinations[9]: $V_{\uparrow\uparrow\uparrow\uparrow}^{\Lambda} = V_{\downarrow\downarrow\downarrow\downarrow}^{\Lambda}$, $V_{\uparrow\downarrow\uparrow\downarrow}^{\Lambda} = V_{\downarrow\uparrow\downarrow\uparrow}^{\Lambda}$, and $V_{\uparrow\downarrow\downarrow\uparrow}^{\Lambda} = V_{\downarrow\uparrow\uparrow\downarrow}^{\Lambda}$. Finally, due to SU(2) symmetry and crossing relation one has:

$$\begin{aligned} V_{\uparrow\uparrow\uparrow\uparrow}^{\Lambda}(k_1, k_2, k_3) &= V_{\uparrow\downarrow\uparrow\downarrow}^{\Lambda}(k_1, k_2, k_3) \\ &\quad - V_{\uparrow\downarrow\uparrow\downarrow}^{\Lambda}(k_1, k_2, k_1 + k_2 - k_3), \quad (3) \\ V_{\uparrow\downarrow\downarrow\uparrow}^{\Lambda}(k_1, k_2, k_3) &= -V_{\uparrow\downarrow\uparrow\downarrow}^{\Lambda}(k_1, k_2, k_1 + k_2 - k_3). \quad (4) \end{aligned}$$

This allows us to consider only one function of three arguments for the vertex: $V_{\uparrow\downarrow\uparrow\downarrow}^{\Lambda}(k_1, k_2, k_3) = V^{\Lambda}(k_1, k_2, k_3)$, all the others spin components being obtained by symmetry.

With these considerations the flow equation for the self energy[2] reads:

$$\frac{d}{d\Lambda}\Sigma^{\Lambda}(k) = -\int_p S^{\Lambda}(p) \left[2V^{\Lambda}(k,p,p) - V^{\Lambda}(k,p,k) \right],$$

$$(5)$$

with $p = (\omega, \mathbf{p})$ and $k = (\nu, \mathbf{k})$. We use the notation $\int_p = T \sum_\omega \int_{\mathbf{p}}$, $\int_{\mathbf{q}} = \int \frac{d\mathbf{q}}{4\pi^2}$ being the normalized integral

over the first Brillouin zone.

$$S^\Lambda = \left. \frac{dG^\Lambda}{d\Lambda} \right|_{\Sigma=\text{const}} \qquad (6)$$

is the single-scale propagator and $G^\Lambda = \left[(G_0^\Lambda)^{-1} - \Sigma^\Lambda\right]^{-1}$ is the full propagator.

The vertex flow equation[2,10] can be written as:

$$\frac{d}{d\Lambda} V(k_1, k_2, k_3) = \mathcal{T}_{\text{pp}}^\Lambda(k_1, k_2, k_3) + \mathcal{T}_{\text{ph}}^\Lambda(k_1, k_2, k_3) + \mathcal{T}_{\text{phc}}^\Lambda(k_1, k_2, k_3), \qquad (7)$$

where:[?]

$$\begin{aligned}
\mathcal{T}_{\text{pp}}^\Lambda(k_1, k_2, k_3) &= -\frac{1}{2} \int_p \mathcal{P}^\Lambda(p, k_1 + k_2 - p) \Big\{ V^\Lambda(k_1, k_2, k_1 + k_2 - p) V^\Lambda(k_1 + k_2 - p, p, k_3) \\
&\qquad + V^\Lambda(k_1, k_2, p) V^\Lambda(p, k_1 + k_2 - p, k_3) \Big\};
\end{aligned} \qquad (8)$$

$$\begin{aligned}
\mathcal{T}_{\text{ph}}^\Lambda(k_1, k_2, k_3) &= -\int_p \mathcal{P}^\Lambda(p, k_3 - k_1 + p) \Big\{ 2 V^\Lambda(k_1, k_3 - k_1 + p, k_3) V^\Lambda(p, k_2, k_3 - k_1 + p) \\
&\qquad - V^\Lambda(k_1, k_3 - k_1 + p, p) V^\Lambda(p, k_2, k_3 - k_1 + p) - V^\Lambda(k_1, k_3 - k_1 + p, k_3) V^\Lambda(k_2, p, k_3 - k_1 + p) \Big\};
\end{aligned} \qquad (9)$$

$$\mathcal{T}_{\text{phc}}^\Lambda(k_1, k_2, k_3) = \int_p \mathcal{P}^\Lambda(p, k_2 - k_3 + p) V^\Lambda(k_1, k_2 - k_3 + p, p) V^\Lambda(p, k_2, k_3). \qquad (10)$$

Here we have defined the quantity:

$$\mathcal{P}^\Lambda(p, p') = G^\Lambda(p) S^\Lambda(p') + G^\Lambda(p') S^\Lambda(p). \qquad (11)$$

For any Λ-dependence so that $G_0^{\Lambda_0} = 0$ the initial condition for the self-and the vertex are[2], respectively, $\Sigma^{\Lambda_0} = 0$ and $V^{\Lambda_0} = U$.

III. VERTEX APPROXIMATION

In order to deal with the frequency and momentum dependence of the vertex, we start by decomposing the vertex as follows:

$$V^\Lambda(k_1, k_2, k_3) = U - \phi_{\text{p}}^\Lambda(k_1 + k_2; k_1, k_3) + \phi_{\text{m}}^\Lambda(k_3 - k_1; k_1, k_2) + \frac{1}{2} \phi_{\text{m}}^\Lambda(k_2 - k_3; k_1, k_2) - \frac{1}{2} \phi_{\text{c}}^\Lambda(k_2 - k_3; k_1, k_2), \quad (12)$$

where the physical meaning of each ϕ channel will be understood by the structure of its flow equations:

$$\dot{\phi}_{\text{p}}^\Lambda(Q; k_1, k_3) = -\mathcal{T}_{\text{pp}}^\Lambda(k_1, Q - k_1, k_3), \qquad (13)$$

$$\dot{\phi}_{\text{c}}^\Lambda(Q; k_1, k_2) = -2\mathcal{T}_{\text{ph}}^\Lambda(k_1, k_2, Q + k_1) + \mathcal{T}_{\text{phc}}^\Lambda(k_1, k_2, Q + k_1), \qquad (14)$$

$$\dot{\phi}_{\text{m}}^\Lambda(Q; k_1, k_2) = \mathcal{T}_{\text{phc}}^\Lambda(k_1, k_2, Q + k_1), \qquad (15)$$

where $Q = (\Omega, \mathbf{Q})$ is a frequency and momentum transfer.

Following Refs. 10,11, we address first the momentum dependence. To this end, we introduce a decomposition of the unity by means of a set of orthonormal form factors for the two fermionic momenta $\{f_l(\mathbf{k})\}$ obeying the completeness relation:

$$\int_{\mathbf{k}} f_l(\mathbf{k}) f_m(\mathbf{k}) = \delta_{l,m}. \qquad (16)$$

The procedure outlined here is described in detail, e.g., in Ref. 12

We can then project each channel on a subset of form factors, whose choice is physically motivated[10]. Let us stress that the if one could keep all the form factors the expansion would be exact.

For the pairing channel we keep only $f_s(\mathbf{k}) = 1$ and

$$f_d(\mathbf{k}) = \cos k_x - \cos k_y:$$

$$\phi_{\rm p}^\Lambda(Q; k_1, k_3) = \mathcal{S}_{\mathbf{Q}}^{\Omega; \nu_1, \nu_3} + \\ f_d\left(\frac{\mathbf{Q}}{2} - \mathbf{k}_1\right) f_d\left(\frac{\mathbf{Q}}{2} - \mathbf{k}_3\right) \mathcal{D}_{\mathbf{Q}}^{\Omega; \nu_1, \nu_3}. \tag{17}$$

The instability in the channel $\mathcal{S}$ is associated to s-wave superconductivity, while $\mathcal{D}$ to d-wave superconductivity.

For the charge and magnetic channels we restrict ourselves to $f_s(\mathbf{k}) = 1$ only:

$$\phi_{\rm c}^\Lambda(Q; k_1, k_2) = \mathcal{C}_{\mathbf{Q}}^{\Omega; \nu_1, \nu_2}, \tag{18}$$

$$\phi_{\rm m}^\Lambda(Q; k_1, k_2) = \mathcal{M}_{\mathbf{Q}}^{\Omega; \nu_1, \nu_2}, \tag{19}$$

corresponding to instabilities in the charge and magnetic channels, respectively (for notation simplicity we omit the Λ-dependences of the channel functions $\mathcal{S}$, $\mathcal{D}$, $\mathcal{C}$ and $\mathcal{M}$).

Let us stress that for each channel we have defined *its own* frequency notation, consisting of one frequency corresponding to the frequency transferred in the specific channel and two remaining independent fermionic frequencies. At finite temperature the frequency transfer, being a sum or a difference of two fermionic Matsubara frequencies, is a bosonic Matsubara frequency.

The choice of the mixed notation is the most natural[13] since the transferred momentum and frequency play a special role in the diagrammatics. Indeed, on the one hand, it is the only dependence generated in second order perturbation theory and the main dependence in finite order perturbation theory. On the other hand, this notation is convenient to express the Bethe-Salpeter equations[9], which are deeply related to parquet-approximations and fRG.

In the fRG literature[10,11,14], where the fermionic frequency dependence is neglected, the channel functions above are sometimes interpreted as bosonic exchange propagators. Such an interpretation is missing in the presence of all frequencies.

Although one expects a leading dependence in the bosonic frequency, in particular in the weak coupling regime, we will see that in some cases the dependence on fermionic frequencies can become strong and not negligible.

The flow equations for the channels $\mathcal{S}$, $\mathcal{D}$, $\mathcal{C}$ and $\mathcal{M}$ can be derived from the projection onto form factors of Eq. (8)-(10):

$$\dot{\mathcal{S}}_{\mathbf{Q}}^{\Omega; \nu_1, \nu_3} = -\int_{\mathbf{k}_1, \mathbf{k}_3} \mathcal{T}_{\rm pp}(k_1, Q - k_1, k_3); \tag{20}$$

$$\dot{\mathcal{D}}_{\mathbf{Q}}^{\Omega; \nu_1, \nu_3} = -\int_{\mathbf{k}_1, \mathbf{k}_3} f_d\left(\frac{\mathbf{Q}}{2} - \mathbf{k}_1\right) f_d\left(\frac{\mathbf{Q}}{2} - \mathbf{k}_3\right) \\ \mathcal{T}_{\rm pp}(k_1, Q - k_1, k_3); \tag{21}$$

$$\dot{\mathcal{C}}_{\mathbf{Q}}^{\Omega; \nu_1, \nu_2} = \int_{\mathbf{k}_1, \mathbf{k}_2} \mathcal{T}_{\rm phc}(k_1, k_2, Q + k_1) \\ - 2\mathcal{T}_{\rm ph}(k_1, k_2, k_2 - Q); \tag{22}$$

$$\dot{\mathcal{M}}_{\mathbf{Q}}^{\Omega; \nu_1, \nu_2} = \int_{\mathbf{k}_1, \mathbf{k}_2} \mathcal{T}_{\rm phc}(k_1, k_2, Q + k_1). \tag{23}$$

The final equations are then obtained by substituting the decomposition (12) into the equations above, and using trigonometric eventualities. As an example we report here the equation for the magnetic channel, while the expression for the other channels are reported in the Appendix:

$$\dot{\mathcal{M}}_{\mathbf{Q}}^{\Omega; \nu_1, \nu_2} = \sum_\nu L_{\mathbf{Q}}^{\Omega; \nu_1, \nu} P_{\mathbf{Q}}^{\Omega, \nu} L_{\mathbf{Q}}^{\Omega; \nu, \nu_2 - \Omega}, \tag{24}$$

(the Λ-dependence is implicit), with:

$$P_{\mathbf{Q}}^{\Omega; \nu} = \int_{\mathbf{P}} G_{\mathbf{p}}^\Lambda(\nu) S_{\mathbf{Q}+\mathbf{p}}^\Lambda(\Omega+\nu) + G_{\mathbf{Q}+\mathbf{p}}^\Lambda(\Omega+\nu) S_{\mathbf{p}}^\Lambda(\nu), \tag{25}$$

and:

$$L_{\mathbf{Q}}^{\Omega; \nu_1, \nu_2} = U + \mathcal{M}_{\mathbf{Q}}^{\Omega; \nu_1, \nu_2} \\ + \int_{\mathbf{p}} \Big\{ -\mathcal{S}_{\mathbf{p}}^{\nu_1+\nu_2; \nu_1, \nu_1+\Omega} \\ -\frac{1}{2} \mathcal{D}_{\mathbf{p}}^{\nu_1+\nu_2; \nu_1, \nu_1+\Omega} [\cos(Q_x) + \cos(Q_y)] \\ +\frac{1}{2} \left[\mathcal{M}_{\mathbf{p}}^{\nu_2-\nu_1-\Omega; \nu_1, \nu_2} - \mathcal{C}_{\mathbf{p}}^{\nu_2-\nu_1-\Omega, \nu_1, \nu_2} \right] \Big\} \tag{26}$$

Let us notice that after the momentum integrals in P and L are performed, the right hand side can be expressed as a matrix-matrix multiplication in frequency space, where Ω and $\mathbf{Q}$ appear as parameters.

After this decomposition, the evaluation of vertex-flow equation, depending on three momenta and three momenta is reduced to the flow of the four functions $\mathcal{S}$, $\mathcal{S}$, $\mathcal{C}$, $\mathcal{M}$ each of them depending on three frequencies and one momentum only. In order to compute these equations numerically we needed to discretize the momentum dependence on patches covering the Brillouin zone and to truncate the frequency dependence to some maximal frequency value. More details about this are given in the Appendix. Here let us stress, however, that an approximation on the momentum space using a form factor decomposition gave us results much more controllable than a similar approximation[15] in frequency space. In fact the results obtained with this latter approximation turned out to depend sensitively on the way the projection was performed, and hence we discarded it, as we will discuss later.

A. Cutoff choice

To use the flow equations defined above we need to specify the Λ-dependence of the non interacting propagator, often referred to as *cutoff*, in connection to the scale-separation of the renormalization group. In the rest of the paper we have used two different cutoffs.

For most our calculations we have used the *Interaction cutoff*, introduced in Ref. 16:

$$G_0^\Lambda(k) = \Lambda G_0(k) = \frac{\Lambda}{i\nu - \mu - \varepsilon_{\mathbf{k}}}, \qquad (27)$$

Where the scale-parameter Λ flows from 0 to 1, and with $\varepsilon_{\mathbf{k}} = -2t[\cos(k_x) + \cos(k_y)] - 4t'\cos(k_x)\cos(k_y)$. μ is the chemical potential needed to fix the occupation at a given value n. ν is a fermionic Matsubara-frequency: $\nu = \frac{\pi}{\beta}(2m+1)$, $m \in \mathbb{Z}$. $\beta = 1/T$ is the inverse temperature. Correspondingly the interacting Green's function reads:

$$G^\Lambda(k) = \frac{\Lambda}{i\nu - \varepsilon_{\mathbf{k}} - \mu^\Lambda - \Lambda\Sigma^\Lambda(k)} \qquad (28)$$

We have introduced a Λ-dependent chemical potential to maintain the occupation fixed during the flow: the chemical potential becomes a functional of the flowing self-energy: $\mu^\Lambda = \mu[\Sigma^\Lambda]$, whose value is found by solving the equation:

$$n = \int_p e^{i\omega 0^+} \frac{G^\Lambda(p)}{\Lambda}. \qquad (29)$$

The main advantage of the interaction cutoff is that the Λ-dependent action can be interpreted[16] as the physical action of the system with rescaled interaction $\tilde{U}^\Lambda = \Lambda^2 U$. For our purposes, we do not need to worry about the fact that this cutoff is not scale-selective, and hence does not regularize possible divergences in the bubbles. Indeed, in the finite-temperature case, T acts itself as an infrared cutoff. Furthermore it has been shown in Ref. 17 that, in the context of the single-impurity Anderson model, the vertex-structures do not depend qualitatively on the cutoff-choice, and, at weak-coupling, depend on it only very little quantitatively.

As a benchmark for the robustness of our results on the cutoff-choice, we have used a soft version of the *frequency selective cutoff* defined[18] by:

$$G_0^\Lambda(k) = \frac{1}{i\,\mathrm{sign}\sqrt{\nu^2 + \Lambda^2} - \mu - \varepsilon_{\mathbf{k}}}, \qquad (30)$$

with $\Lambda_0 = \infty$ and $\Lambda_f = 0$. Also in this case we have performed our calculations at fixed occupation.

IV. RESULTS

A. Frequency dependence of Vertex

- Forward scattering problem seen by Salmhofer

- Show phase diagram, Λ_{cri} vs $x = 1 - n$, with and without Σ (for differenct t')

- Self energy "solve" the problem of charge instability.

- Suggestion: The charge problem exists also at van Hove filling where, according to the literature, the Σ has no effect when Karrasch approximation is taken into account.

- Colorplots: Mag and Charge channel

B. Forward scattering problem

- Introduce perpendicular ladder (PL) for charge.

- Colorplot of charge in PL.

- Discuss the role of the Bubble at $\mathbf{Q} = (0,0)$ and plot it as a function of ν.

C. Self energy effects

- With self energy feedback, we didn't find any charge instability problem for any parameters range studied.

- Plot of the Fermi surface based patch scheme.

- Plot of $\Sigma(i\omega)$ at $\mathbf{k} = (\pi, 0)$, $\mathbf{k} = \mathbf{k}_{HS}$ and $\mathbf{k} = (\pi/2, \pi/2)$ in frequency space.

- Plot of $Z_{\mathbf{k}}$

- Plot of occupation with and without Σ

V. CONCLUSIONS

Conclusions...

Acknowledgments

We thank for valuable discussions. This research was supported by.

VI. APPENDICES

Appendices...

[1] J. Hubbard. Electron Correlations in Narrow Energy Bands. *Proc. R. Soc. A*, 276:238–257, November 1963.

[2] W. Metzner, M. Salmhofer, C. Honerkamp, V. Meden, and K. Schönhammer. Functional renormalization group approach to correlated fermion systems. *Rev. Mod. Phys.*, 84:299–352, January 2012.

[3] C. Platt, W. Hanke, and R. Thomale. Functional renormalization group for multi-orbital fermi surface instabilities. *Advances in Physics*, 62(4-6):453–562, 2013.

[4] C. Wetterich. Exact evolution equation for the effective potential. *Physics Letters B*, 301:90–94, February 1993.

[5]

[6] Binz, B., Baeriswyl, D., and Douçot, B. Wilson's renormalization group applied to 2d lattice electrons in the presence of van hove singularities. *Eur. Phys. J. B*, 25(1):69–87, 2002.

[7] B. Binz, D. Baeriswyl, and B. Douçot. Weakly interacting electrons and the renormalization group. *Annalen der Physik*, 12(11-12):704–736, 2003.

[8] F. B. Kugler and J. von Delft. Multiloop functional renormalization group that sums up all parquet diagrams. *ArXiv e-prints*, March 2017.

[9] G. Rohringer, A. Valli, and A. Toschi. Local electronic correlation at the two-particle level. *Phys. Rev. B*, 86(12):125114, September 2012.

[10] C. Husemann and M. Salmhofer. Efficient parametrization of the vertex function, Ω scheme, and the t,t$'$ Hubbard model at van Hove filling. *Phys. Rev. B*, 79(19):195125, May 2009.

[11] C. Husemann, K.-U. Giering, and M. Salmhofer. Frequency-dependent vertex functions of the (t, t') hubbard model at weak coupling. *Phys. Rev. B*, 85:075121, Feb 2012.

[12] J. Lichtenstein, D. Sánchez de la Peña, D. Rohe, E. Di Napoli, C. Honerkamp, and S.A. Maier. High-performance functional renormalization group calculations for interacting fermions. *Computer Physics Communications*, 213:100 – 110, 2017.

[13] N. Wentzell, G. Li, A. Tagliavini, C. Taranto, G. Rohringer, K. Held, A. Toschi, and S. Andergassen. High-frequency asymptotics of the vertex function: diagrammatic parametrization and algorithmic implementation. *ArXiv e-prints*, October 2016.

[14] K.-U. Giering and M. Salmhofer. Self-energy flows in the two-dimensional repulsive Hubbard model. *Phys. Rev. B*, 86(24):245122, December 2012.

[15] C. Karrasch, R. Hedden, R. Peters, T. Pruschke, K. Schönhammer, and V. Meden. A finite-frequency functional renormalization group approach to the single impurity Anderson model. *J. Phys.: Condens. Matter*, 20:H5205, August 2008.

[16] C. Honerkamp, D. Rohe, S. Andergassen, and T. Enss. Interaction flow method for many-fermion systems. *Phys. Rev. B*, 70(23):235115, December 2004.

[17] Nils Wentzell, Serge Florens, Tobias Meng, Volker Meden, and Sabine Andergassen. Magneto-electric spectroscopy of andreev bound states in josephson quantum dots. May 2016.

[18] A. Eberlein. Fermionic two-loop functional renormalization group for correlated fermions: Method and application to the attractive Hubbard model. *Phys. Rev. B*, 90(11):115125, September 2014.

[19] The equation for the particle-particle channel is slightly different from the one usually reported in fRG, see, e.g., Ref. 10. This is because we took $V^\Lambda = V^\Lambda_{\uparrow\downarrow\uparrow\downarrow}$ instead of $V^\Lambda = V^\Lambda_{\uparrow\downarrow\downarrow\uparrow}$.